In Situ Synchrotron X-ray Powder Diffraction Studies of Crystallization of Microporous Aluminophosphates and Me^{2+}-Substituted Aluminophosphates

A. Nørlund Christensen,*,† Torben R. Jensen,‡ Poul Norby,§ and Jonathan C. Hanson▽

Department of Inorganic Chemistry, Aarhus University, DK-8000 Aarhus C, Denmark, Department of Chemistry, Odense University, DK-5230 Odense M, Denmark, Department of Chemistry, SUNY−Stony Brook, Stony Brook, New York 11794-3400, and Chemistry Department, Brookhaven National Laboratory, Upton, New York 11973

Received January 27, 1998. Revised Manuscript Received March 13, 1998

In situ synchrotron X-ray powder diffraction was used to study the crystallization of microporous aluminophosphate and of Mg^{2+}-, Mn^{2+}-, Co^{2+}-, and Zn^{2+}-substituted aluminophosphates. The gels contained the templates 2-(diethylamino)ethanol, di-*n*-propylamine, triethylamine, and tripropylamine and were heated in quartz glass capillaries at temperatures up to 200 °C. The main crystalline reaction products formed were $AlPO_4$ (tridymite type), APO-5 (AFI), APO-11 (AEL), MgAPO-5 (AFI), MnAPO-5 (AFI), CoAPO-5 (AFI), ZnAPO-39 (ATN), and ZnAPO-47 (CHA). A kinetic analysis of the crystallization of MnAPO-5 (AFI) and ZnAPO-47 (CHA) was performed using isothermal in situ synchrotron X-ray powder diffraction data. The apparent activation energies for the hydrothermal nucleation of MnAPO-5 (AFI) and ZnAPO-47 (CHA) were 161(6) and 112(3) kJ/mol, respectively. The crystallization of MnAPO-5 could be modeled using a first-order expression giving an apparent activation energy of the crystal growth of 81(6) kJ/mol. The crystallization of ZnAPO-47 was more complex, and the crystallization curves could not be described using simple kinetic expressions.

Introduction

Since the discovery of the microporous aluminophosphate molecular sieves by Wilson et al.,[1] a large number of aluminophosphate-based framework structures have been synthesized and characterized. Among these are the catalytically active MAPO's,[2] where aluminum in the framework is partly substituted by the metals Mg, Mn, Co, and Zn. The microporous aluminophosphate-based compounds are made at hydrothermal conditions from amorphous aluminophosphate gels containing organic template molecules. Parameters in the synthesis can be as follows: molar ratios of components in the gels; molecular size of the organic template; choice of the Me^{2+} ions to substitute the Al^{3+} ions; pH; nucleation and aging of the gels; temperature and time of the hydrothermal reaction. Although papers have been published on the synthesis of MAPO's,[3−8] little is known about the rate of formation of the MAPO's at the hydrothermal conditions. However, in situ synchrotron X-ray powder diffraction investigations can be used to follow phase transitions or chemical reactions in a heterogeneous system where at least one component should be a crystalline compound.[9−20] Time-resolved or in situ powder diffraction has thus been developed to study chemical reactions on heterogeneous catalysis,[9] reactions of calcium aluminates with water,[10] and hydrothermal synthesis of MAPO's.[11] In situ powder

* Correspondence to Dr. A. Nørlund Christensen. Tel: +45 8942 3894. Fax: +45 8619 6199. E-mail: anc@kemi.aau.dk.
† Aarhus University.
‡ Odense University.
§ SUNY−Stony Brook. Present address: Aarhus University.
▽ Brookhaven National Laboratory.

(1) Wilson, S. T.; Lok, B. M.; Flanigen, E. M. U.S. Patent 4310440, 1982.
(2) Flanigen, E. M.; Lok, B. M.; Patton, R. L.; Wilson, S. T. *Stud. Surf. Sci. Catal.* **1986**, *28*, 103.
(3) Ojo, A. F.; McCusker, L. B. *Zeolites* **1991**, *11*, 460.
(4) Akolekar, D. B.; Kaliaguine, S. K. *Zeolites* **1994**, *14*, 620.
(5) Shea, W.-L.; Borade, R. B.; Clearfield, A. *J. Chem. Soc., Faraday Trans.* **1993**, *89*, 3143.
(6) Akolekar, D. B.; Kaliaguine, S. K. *J. Chem. Soc., Faraday Trans.* **1993**, *89*, 4141.
(7) Akolekar, D. B. *J. Catal.* **1993**, *143*, 227.
(8) Han, S.; Smith, J. V.; Pluth, J. J.; Richardson, J. W., Jr., *Eur. J. Mineral* **1990**, *2*, 787.
(9) Clausen, B. S.; Steffensen, G.; Fabius, B.; Villadsen, J.; Feidenhans'l, R.; Topsøe, H. *J. Catal.* **1991**, *132*, 524.
(10) Christensen, A. N.; Lehmann, M. S. *J. Solid State Chem.* **1984**, *51*, 196.
(11) Norby, P. *Mater. Sci. Forum* **1996**, *228−231*, 147.
(12) Norby, P.; Christensen, A. N.; Hanson, J. C. In *Zeolites and Related Microporous Materials: State of the Art 1994. Studies in Surface Science and Catalysis*; Weitkamp, J., Karge, H. G., Pfeifer, H., Hölderich, W., Eds.; 1994; Vol. 84, p 179.
(13) Christensen, A. N.; Norby, P.; Hanson, J. C. *Acta Chem. Scand.* **1997**, *51*, 249.
(14) Christensen, A. N.; Norby, P.; Hanson, J. C. *J. Microporous Mater.*, accepted.
(15) Cheetham, A. K.; Mellot, C. F. *Chem. Mater.* **1997**, *9*, 2269.
(16) Norby, P. *J. Appl. Crystallogr.* **1997**, *30*, 21.
(17) Christensen, A. N.; Norby, P.; Hanson, J. C.; Shimada, S. *J. Appl. Crystallogr.* **1996**, *29*, 265.
(18) Norby, P. *J. Am. Chem. Soc.* **1997**, *119*, 5215.
(19) Gualtieri, A.; Norby, P.; Artioli, G.; Hanson, J. *Microporous Mater.* **1997**, *9*, 189.
(20) Francis, R. J.; Price, S. J.; O'Brien, S.; Fogg, A. M.; O'Hare, D.; Loiseau, T.; Férey, G. *Chem. Commun.* **1997**, 521.

S0897-4756(98)00049-0 CCC: $15.00
Published on Web 04/29/1998

Table 1. Composition Listed as Molar Ratios of Gels Used for in Situ Experiments[a]

name of gel	template	MeO	Al_2O_3	P_2O_5	H_2O	pH of gel	hydrothermal reaction product
AP1	TEA, 1.10		0.33	1.00	47.00	5.00	$AlPO_4$, tridymite
AP2	TEA, 1.10		0.33	1.00	22.00	4.53	$AlPO_4 \cdot 2H_2O$, variscite
AP3	TEA, 0.41		1.00	1.00	52.00	5.37	APO-5, AFI
AP6	DPA, 1.00		1.00	1.00	40.00	3.00	APO-11, AEL, and $AlPO_4$, tridymite
		MgO					
MgAP1	TEA, 1.10	0.21	0.30	1.00	23.00	4.64	MgAPO-5, AFI
MgAP3	TEA, 1.00	0.21	0.80	1.00	52.00	5.78	MgAPO-5, AFI, and MgAPO-47, CHA
MgAP4	DPA, 1.00	0.40	0.80	1.00	40.00	4.00	MgAPO-11, AEL
MAPO-D	TPA, 1.91	0.17	0.96	1.00	25.20	6.73	MgAPO-5, AFI
		MnO					
MnAP2	DEAE, 0.81	0.34	0.99	1.00	29.00	5.87	MnAPO-5, AFI
MnAP3	TEA, 1.10	0.21	0.30	1.00	23.00	4.87	$AlPO_4$, tridymite
MnAP4	TEA, 1.10	0.21	0.30	1.00	32.00	4.42	$AlPO_4$, tridymite
MnAP5	TEA, 1.60	0.21	0.80	1.00	52.00	4.97	MnAPO-5, AFI
		CoO					
CoAP1	TEA, 1.60	0.16	0.41	1.00	45.00	4.50	$AlPO_4$, tridymite
		ZnO					
ZnAP1	DPA, 1.00	0.40	0.80	1.00	40.00	5.13	ZnAPO-36, ATS, and ZnAPO-39, ATN
ZnAP3	TEA, 1.56	0.40	0.36	1.00	106.00	3.96	ZnAPO-5, AFI, and $Zn_3(PO_4)_2 \cdot 4H_2O$
ZnAP5	TEA, 1.73	0.21	0.36	1.00	48.00	4.58	ZnAPO-47, CHA, and $AlPO_4$, berlinite
ZnAP6	TEA, 1.10	0.21	0.30	1.00	23.00	4.78	$ZnAPO_4$-47, CHA, and $AlPO_4$, berlinite
ZnAP7	TEA, 1.10	0.21	0.30	1.00	32.00	4.37	ZnAPO-5, CHA, and $AlPO_4$, berlinite
ZnAP8	TEA, 1.10	0.21	0.80	1.00	52.00	5.49	$ZnAPO_4$, CHA
ZnAP9	DPA, 1.00	0.40	0.80	1.00	40.00	3.50	ZnAPO-36, ATS, and ZnAPO-39, ATN

[a] The templates used were 2-(diethylamino)ethanol, DEAE; di-*n*-propylamine, DPA; triethylamine, TEA; and tripropylamine, TPA.

diffraction investigation of the synthesis of microporous Co-, Mg-, Mn-, and ZnMAPO's showed[12−14] that precursor phases could be detected and that the formation of the MAPO's depended in a complicated manner upon choice of template and substituting Me^{2+} ion and on experimental conditions as molar ratios of components in the gels and on heating rate and reaction temperatures applied.

To obtain kinetic information about the formation of microporous aluminophosphates and to investigate the dependence of crystallization and nucleation rates upon substitution and template, a series of isothermal and nonisothermal hydrothermal syntheses were performed and the crystallization was followed by time-resolved in situ synchrotron X-ray powder diffraction.

Experimental Section

Sample Preparation. The chemicals used in the preparation of the gels were 85% H_3PO_4 (Merck); pseudo-boehmite (Catapal B, Vista Chemical Co.); and aluminum isopropoxide (98%), $Mg(CH_3COO)_2 \cdot 4H_2O$, $Mn(CH_3COO)_2 \cdot 4H_2O$, $Zn(CH_3COO)_2 \cdot 2H_2O$, 2-(diethylamino)ethanol (DEAE), di-*n*-propylamine (DPA), triethylamine (TEA), and tripropylamine (TPA), all from Aldrich. The compositions of the gels are listed in Table 1 as molar ratios. For each gel a charge was prepared sufficiently large for all synthesis and diffraction experiments performed, approximately 50−100 mL of each. The procedure for the preparation of the gels using pseudo-boehmite as the Al source has been reported previously.[13] Using aluminum isopropoxide the following procedure was applied: The Al source was stirred with 25−30 mL of deionized water for 15 min, and then 85% phosphoric acid was added. The mixture was stirred for at least 15 min until a clear solution was obtained. The Me^{2+} salt in a solution of 15−20 mL of deionized water was added dropwise with continuous stirring. Then the mixture was cooled in an ice bath, the organic amine was added dropwise with continuous stirring, and deionized water was eventually added to adjust the molar ratios of the gel to those listed in Table 1. The gel was further stirred for 1−2 h to obtain homogeneity. The pH of the gel was measured using a pH meter, and the charges so obtained were stored at room temperature in flasks of polyethylene.

Preliminary hydrothermal experiments were made at 170 °C with samples of the gels charged in Teflon containers in pressure vessels, and the crystalline reaction products so obtained were identified from their X-ray patterns (Table 1).

In Situ Measurements. The in situ synchrotron X-ray powder diffraction investigations of the gels were made at the Huber diffractometer at beam line X7B at NSLS, Brookhaven National Laboratory. The samples were kept in 0.5- or 0.7-mm diameter quartz glass capillaries at an internal pressure of up to 25 atm. With a wall thickness of only 0.01 mm, quartz glass capillaries can usually withstand an internal pressure of up to 50 atm, although it depends on the quality of the particular capillary. Because of the potential risk of breakage, safety glasses must be worn. However, because of the very small volume of the reaction cell, the hazards involved are minimal. The capillaries were heated with a stream of hot air, and the temperature was monitored with a thermocouple placed in the stream of hot air and 1 mm from the capillaries. The relation between the temperature in the capillaries and the monitored temperature was obtained by measurement of the unit cell parameters of a sample of microcrystalline silver powder prepared by thermal decomposition of silver carbonate. Powder patterns of a sample of powdered silver housed in a 0.5-mm diameter quartz capillary were recorded at different temperatures. The unit cell parameters of silver were then calculated using a least-squares fit, and from the thermal expansion data for silver,[21] a calibration curve of temperature in the capillaries vs monitored temperature was derived. The powder patterns were recorded on a translating imaging plate system[16] using Fuji imaging plates. The continuous powder diffraction traces on the imaging plates are very adequate for a detailed study of phase transition and of transformation of amorphous samples to crystalline products. The wavelength used was 1.3808(1) Å, calculated from a powder pattern of a LaB_6 standard (NIST SRM 660a, a = 4.156 95 Å). Bragg reflections were typically recorded out to $\sin\theta/\lambda = 0.45$, and the crystalline compounds formed were identified from their X-ray powder patterns. Further details of the in situ methods using X-ray synchrotron powder diffraction have been reported previously.[16−18]

(21) Meyer, R. J. *Gmelins Handbuch der Anorganischen Chemie*; 8. Auflage, Silber, Teil A2; Verlag Chemie GmbH: Weinheim, 1970; p 217.

Table 2. Results of in Situ Experiments with APO and MAPO Gels[a]

expt no.	gel	precursor	impurity	product
1	AP1	APO-5, AFI		$AlPO_4$, tridymite
2	AP2	APO-5, AFI		$AlPO_4$, tridymite
3	AP3		$AlPO_4$, tridymite	APO-5, AFI
4	AP6	APO-54, VPI	$AlPO_4$, tridymite	APO-11, AEL
5	MgAP1		MgAPO-47, CHA	MgAPO-5, AFI
6	MgAP3			MgAPO-5, AFI
7	MgAP4		MgAPO-11, AEL	MgAPO-39, ATN and MgAPO-5, AFI
8	MAPO-D	Mg-sinkankasite		MgAPO-36, ATS
9	MnAP2			MnAPO-5, AFI
10	MnAP3			MnAPO-5, AFI
11	MnAP4	MnAPO-5, AFI		$AlPO_4$, tridymite
12	MnAP5			MnAPO-5, AFI
13	CoAP1			CoAPO-5, AFI
14	ZnAP1		ZnAPO-36, ATS[b]	ZnAPO-39, ATN
15	ZnAP3		ZnAPO-5, AFI[b]	ZnAPO-47, CHA
16	ZnAP5		ZnAPO-5, AFI[b]	ZnAPO-47, CHA
17	ZnAP6			ZnAPO-47, CHA
18	ZnAP7		ZnAPO-5, AFI	ZnAPO-47, CHA
19	ZnAP8			ZnAPO-47, CHA
20	ZnAP9		ZnAPO-36, ATS[b]	ZnAPO-39, ATN

[a] Names and structure codes are listed for precursor, impurity, and product phases. [b] An additional impurity, which could not be identified, was present in these experiments.

Results

The preliminary hydrothermal synthesis made at 170 °C in Teflon-lined pressure vessels gave an idea of which crystalline reaction products could be expected in the in situ experiments. The samples were kept at 170 °C for 6 or 18 h. The crystalline reaction products observed in the preliminary synthesis are in general the same as those found in the in situ experiments. However, for the Zn^{2+}-substituted gels, the main product in the 18-h synthesis was often $AlPO_4$, berlinite, but ZnAPO-47, CHA, was obtained in the 6-h synthesis. For the aluminophosphate gel AP2, the hydrothermal synthesis gave the product $AlPO_4 \cdot 2H_2O$, variscite, and the in situ experiment gave the reaction product $AlPO_4$, tridymite (Table 2). The difference between the results obtained in the two sets of experiments, the hydrothermal synthesis in Teflon-lined pressure vessels and the in situ experiments in quartz glass capillaries, may be ascribed to the fact that the heat treatments of the gels in the two series of experiments are not identical, and the gels are in contact with two different container surfaces. For the gels the ripening and nucleation processes are not necessarily the same in the two sets of experiments.

Two heating modes were used in the in situ measurements: (i) heating of the gels from room temperature to 200 °C at a constant heating rate, typically 1.5 °C h^{-1} (temperature ramp), and (ii) fast heating of the gels to a temperature between 100 and 200 °C and keeping this temperature for 2 h (isothermal). The information stored on the imaging plates was converted to powder patterns which were plotted as a stack of patterns. The first heating mode was used to get an overall view of the products formed in the crystallization of the gels. The latter heating mode was used to obtain isothermal data for kinetic investigations, e.g., extraction of apparent activation energies of the formation of two MAPO's.

Temperature Ramp. The results of the in situ experiments using a temperature ramp are listed in Table 2. The compounds listed as products are the main crystalline phases in the reaction mixtures, and the impurities are present in minor quantities. The compounds listed as precursors are formed during the heating of the samples but are completely consumed and are thus not present in the products. Examples of stacks of powder patterns obtained from the investigation will be shown below.

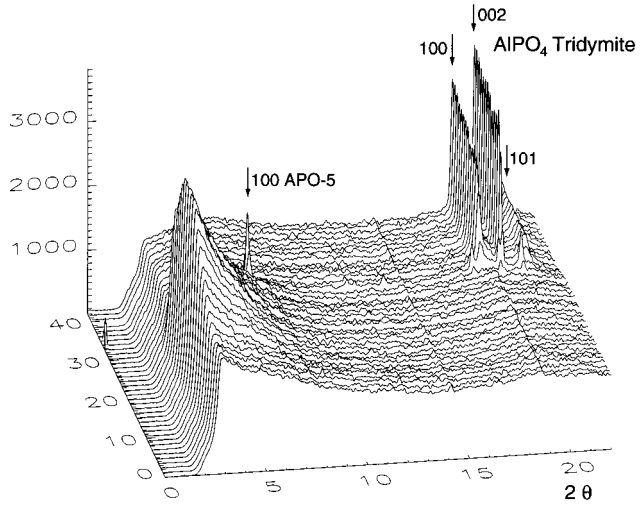

Figure 1. Stack of powder patterns obtained in experiment no. 2 when heating the aluminophosphate gel from room temperature to 200 °C. The reaction product is $AlPO_4$, tridymite type.

Figure 1 displays the powder patterns obtained in experiment no. 2 when heating the aluminophosphate gel from room temperature to 200 °C. APO-5 is formed as a precursor phase and $AlPO_4$, tridymite type, is the reaction product. The amorphous gel creates a background in the patterns in the 2θ range 5−8°, and the background increases in intensity upon heating but disappears rather abruptly when the Bragg reflections of APO-5 and $AlPO_4$ start to appear. The correlation between the decay of the low angle background and the appearance of the Bragg reflections suggests that small particles or aglomerates in the gel are active in the synthesis of the microporous materials. Figure 2 displays the powder patterns obtained in experiment no. 10 when the manganese-substituted aluminophosphate gel MnAP3 is heated from room temperature to 200 °C.

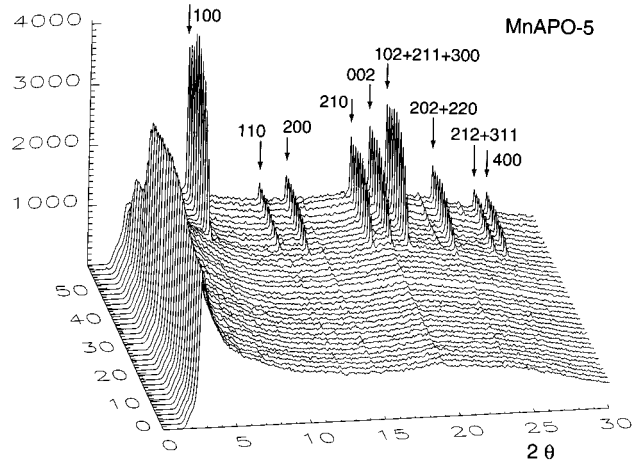

Figure 2. Powder patterns obtained in experiment no. 10 when heating the Mn^{2+}-substituted gel MnAP3 from room temperature to 200 °C. The reaction product is MnAPO-5, AFI.

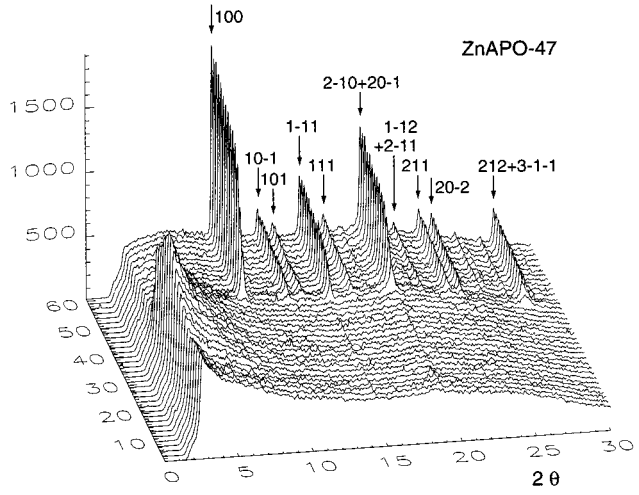

Figure 3. Stack of powder patterns obtained in experiment no. 17 when heating the Zn^{2+}-substituted gel ZnAP6 from room temperature to 200 °C. The reaction product is ZnAPO-47, CHA. The weak Bragg reflections of the patterns without indices all belong to the ZnAPO-47 patterns, so the reaction product is a pure phase.

The crystalline reaction product is MnAPO-5, AFI. Also in this case an amorphous background increases in the 2θ range 5−8° upon heating but is reduced considerably when the Bragg reflections of MnAPO-5 appear in the patterns. Figure 3 shows the powder patterns obtained in experiment no. 17 when heating the zinc substituted aluminophosphate gel ZnAP6 from room temperature to 200 °C. The crystalline reaction product is ZnAPO-47, CHA, and the amorphous background in the 2θ range 5−8° increases upon heating and disappears when the Bragg reflections of ZnAPO-47 appear in the patterns. The changes in intensity of the background in the low angle range 2θ 5−8° indicate that ripening and nucleation processes are taking place during the heating of the gels, and the three gels have been used in a SANS measurement to further study this matter.[22]

Kinetic Investigation of the Crystallization of MnAPO-5, AFI, and ZnAPO-47, CHA. These gels were chosen because they yielded the pure phases ZnAPO-47, CHA, and MnAPO-5, AFI, in the in situ investigation. The capillaries with the gels were heated rapidly to a temperature above 100 °C and kept at these temperatures for up to 2 h.

(22) Christensen, A. N.; Line, C. Experimental Report No. 5-24-41; Institut Laue-Langevin: Grenoble, 1997.

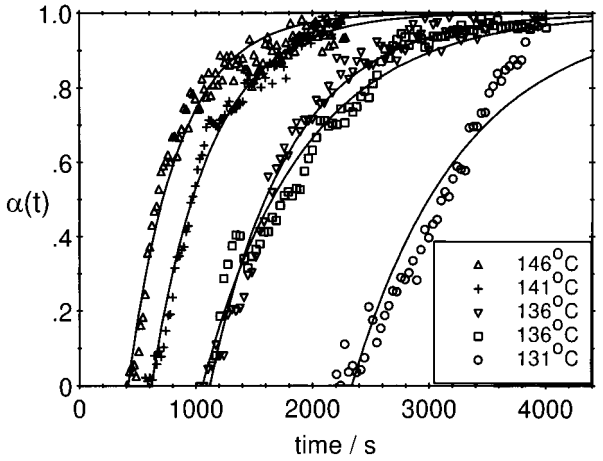

Figure 4. Intensities of Bragg reflections of MnAPO-5, AFI, from in situ crystallization at temperatures of 131, 136, 141, and 146 °C, respectively.

Table 3. Kinetic Data for Crystallization of MnAPO-5[a]

a. Using a First-Order Exponential Kinetic

T (°C)	k (10^{-3} s^{-1})	t_o (s)	t_z (s)	$t_{1/2}$ (s)
146	2.33	417	715	298
141	1.97	617	968	351
136	1.45	1120	1598	478
136	1.15	1055	1657	602
131	1.05	2337	2997	660
E_a (kJ/mol)	81.1	161.2		
ln A	17.3	40.3		

b. Using a Linear Fit to the Observed Data

T (°C)	t_o (s)	t_z (s)	$t_{1/2}$ (s)	$k \cdot t_{1/2}$ (expected value = ln(2) = 0.693)
146	410	666	256	0.596
141	574	969	395	0.778
136	1047	1617	570	0.827
136	1148	1780	632	0.727
131	2180	3131	951	0.999
				0.785 (av value)
E_a (kJ/mol)	159.6		123.0	
ln A	40.0		29.9	

MnAP3 Gel. Figure 4 displays intensities of Bragg reflections vs time. The intensities are normalized to the value 1.0 corresponding to complete crystallization, and each curve represents intensity contributions from the sum of three Bragg reflections, 100, 102, and 211. $\alpha(t)$ thus represents the degree of crystallization. The Avrami equation was fitted to the $\alpha(t)$ data sets which in all cases gave the exponent $n = 1.0$. The crystallization of MnAPO-5, AFI, can thus be expressed by the equation $\alpha(t) = 1 - \exp(-k(t - t_o))$, where k is the rate constant and t_o is the time of the induction period or, rather, the time for nucleation. Table 3a gives the k and t_o values obtained by fitting the first-order expression to the full $\alpha(t)$ data sets, $0 < \alpha(t) < 1$. The observed and calculated crystallization curves of MnAPO-5, AFI, are shown in Figure 4. There is some disagreement between the observed data and the first-order model at 131 °C, possibly because the reaction has not ended completely when the experiment was stopped. The time t_z at which $\alpha(t) = 0.5$ was found from the calculated

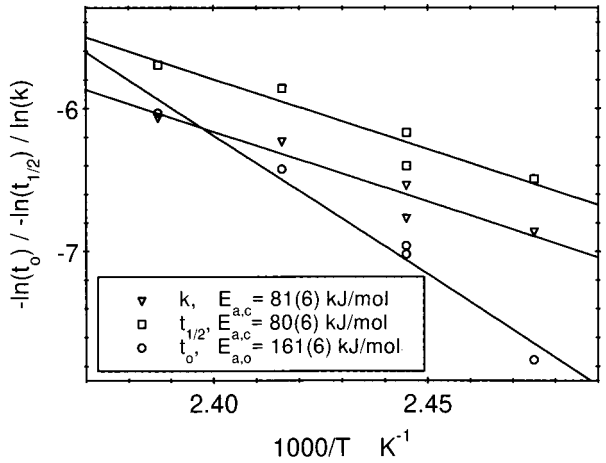

Figure 5. Arrhenius plots for determination of activation energies for the crystallization of MnAPO-5, AFI.

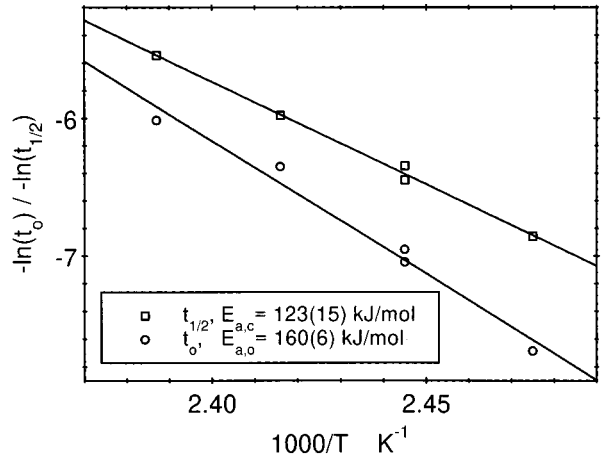

Figure 6. Arrhenius plots for determination of activation energies for the crystallization of MnAPO-5, AFI, using the intervals $0 < \alpha(t) < 0.2$ and $0.4 < \alpha(t) < 0.6$, respectively.

crystallization curves. The time of 50% formation of MnAPO-5, $t_{1/2}$, can be calculated using $t_z = t_o + t_{1/2}$ (the values are in Table 3a). The general Arrhenius expression, $k = A \exp(-E_a/RT)$, was used for the extraction of apparent activation energies for the nucleation and crystal growth (see Figure 5 and Table 3a). The apparent activation energies for the crystal growth calculated from k and $t_{1/2}$ are very similar due to the first-order kinetic model, where $t_{1/2} = \ln(2)/k$. It is observed that the apparent activation energy for the nucleation of 161(6) kJ/mol is higher than the value of 81(6) kJ/mol found for the crystal growth.

To test the agreement between the model and the observed data, t_o and t_z were estimated from the observed crystallization curves using a linear fit in the intervals $0 < \alpha(t) < 0.2$ and $0.4 < \alpha(t) < 0.6$, respectively. This gives a new set of values for $t_{1/2}$ which turns out to be in modest agreement with the first-order model. The results are given in Table 3b together with the product $k \cdot t_{1/2}$ which is expected to be close to the value of ln(2), assuming first-order kinetics. The Arrhenius plot, using t_o, for extraction of the apparent activation energy for the nucleation is shown in Figure 6.

ZnAP6 Gel. The hydrothermal treatment of the gel at different temperatures results in time-dependent particle size of the reaction product. Figure 7 displays

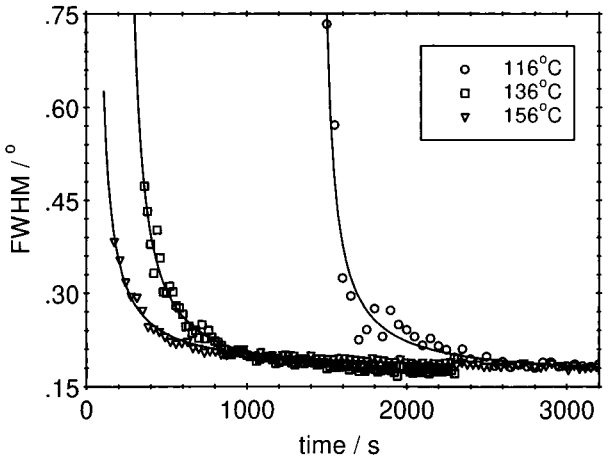

Figure 7. fwhm for the 101 Bragg reflection of ZnAPO-47, CHA, obtained at temperatures of 116, 136, and 156 °C, respectively.

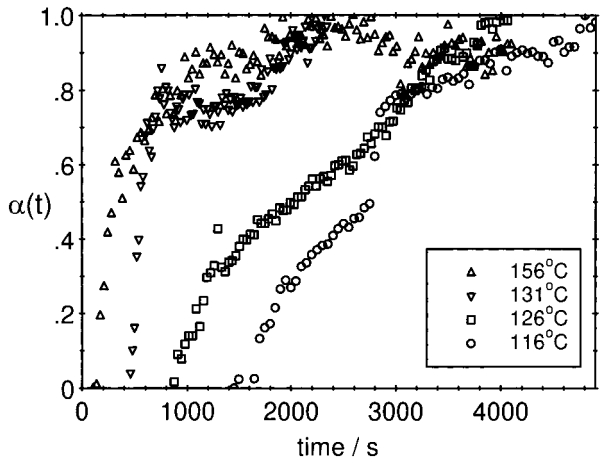

Figure 8. Intensity of Bragg reflections of ZnAPO-47, CHA, from in situ crystallization at temperatures of 116, 126, 131, and 156 °C, respectively.

Table 4. Nucleation Time, t_o, for the Crystallization of ZnAPO-47 Using a Linear Fit to the Observed Data

T (°C)	t_o (s)
156	61
136	296
136	305
131	455
126	787
115	1474
E_a (kJ/mol)	113.0
ln A	27.5

the fwhm for the 101 reflection of ZnAPO-47, CHA, obtained in hydrothermal treatment of the gel at temperatures of 110, 136, and 150 °C, respectively. In all three cases particle growth is observed as a reduction of the fwhm during the time of the experiments. The final values of fwhm at the three temperatures are not significantly different from each other and are close to 0.18°.

Figure 8 displays $\alpha(t)$ vs time for treatment of the ZnAP6 gel at four temperatures. In the same way as above, the normalized sum of the intensities of the Bragg reflections 101, 021, and 211 was used. The crystallization of ZnAPO-47, CHA, is at first proceeding rather rapidly, and after a short period of time the rate of crystallization is reduced. This can also be observed in Figure 3 which shows a stack of powder patterns of

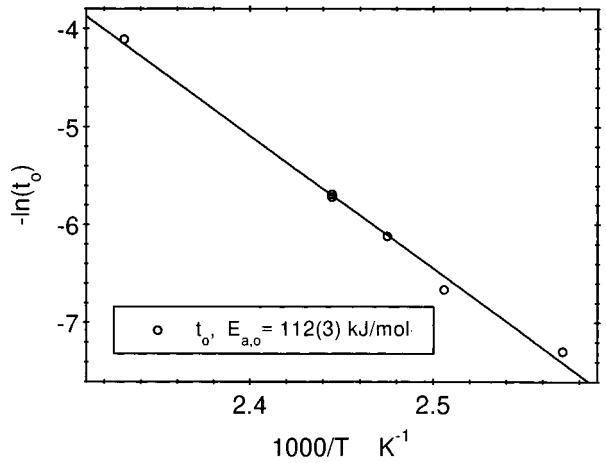

Figure 9. Arrhenius plot for determination of the activation energy for the nucleation process in the crystallization of ZnAPO-47, CHA.

ZnAPO-47, CHA. Avrami expressions do not give good fits to the data. Below approximately 130 °C the crystallization proceeds in two steps with two rate constants. The slower crystallization rate disappears at temperatures over 130 °C. The activation energy for the nucleation process can be estimated from the data listed in Table 4 and from the Arrhenius plot, Figure 9.

Discussion

The in situ experiments performed (Table 2) may be divided into three groups: (a) using APO gels no. 1−4, (b) using Mg-substituted gels no. 5−8, and (c) using transition-metal-substituted gels with Mn, Co, and Zn, no. 9−20. It is well-known that the structure-directing amine strongly influences the composition and structure type of the crystalline product. In the (a) group the microporous aluminophosphates APO-5 and APO-11 were formed in experiments no. 3 and 4, respectively, which had molar ratios of the gels Al_2O_3:P_2O_5 of 1.00:1.00. However, in experiments no. 1 and 2 gels with the Al_2O_3:P_2O_5 ratios 0.33:1.00 were used, and these two experiments resulted in formation of $AlPO_4$ (tridymite type). In the (b) group the microporous reaction products were MgAPO-5, MgAPO-36, and MgAPO-39. These results confirm previous findings.[13,14] In the (c) group the experiments no. 13, 14, and 20 confirm the formation of CoAPO-5[12] and ZnAPO-39[14] reported previously. The Mn-substituted gels result in the formation of MnAPO-5; however, in one case, experiment no. 11, with a gel with a low Al_2O_3:P_2O_5 ratio of 0.30:1.00 the reaction product was $AlPO_4$ of tridymite type. The Zn-substituted gels gave in the experiments no. 15−19 ZnAPO-47 as the main reaction product.

The activation energies for the nucleation of the molecular sieves MnAPO-5, AFI, and ZnAPO-47, CHA, have reasonable values determined from the experimental data. The Avrami equation is widely used for the solution of mediated nucleation and crystal growth reactions. The apparent activation energies extracted using the Avrami equation contain little physical meaning but are important for comparing similar reactions. In situ studies of a synthesis of hydroxysodalite from natural kaolinite activated at different temperatures gave apparent activation energies for the nucleation in the range 71(4)−142(8) kJ/mol.[19] The apparent activation energies presented here have the same order of magnitude. The nucleation process has a larger apparent activation energy than the crystal growth indicating that the nucleation is the rate-limiting step in the synthesis of MnAPO-5, AFI.

The hydrothermal synthesis of the oxyfluorinated gallophosphate, ULM-5, was studied using in situ energy-dispersive X-ray diffraction.[20] The crystallization curves of ULM-5 were similar to those of MnAPO-5 found in this work but were described using an Avrami exponent, $n = 0.4$. Upon modification of the synthesis conditions of ULM-5 (orthophosphoric acid was replaced by phosphorus pentoxide) a crystalline precursor phase was found to exist. The presence of the intermediate phase drastically changed the shape of the ULM-5 crystallization curves to become similar to the ZnAPO-47 crystallization curves (see Figure 8, especially at 116 and 126 °C). This suggests that an amorphous or semicrystalline intermediate stage might exist during the formation of ZnAPO-47. This hypothesis will be investigated further using in situ solid-state MAS NMR at elevated temperature.

Acknowledgment. The Danish Natural Science Research Council and the Danish Technical Research Council have supported this investigation with grants. The synchrotron X-ray measurements were carried out at Brookhaven National Laboratory, supported under Contract DE-AC02-76CH00016 with the U.S. Department of Energy by its Division of Chemical Sciences Office of Basic and Energy Science. Mrs. M. A. Chevallier, Mrs. C. Secher, Mr. A. Lindahl, and Mr. N. J. Hansen are acknowledged for valuable assistance.

CM980049S